# Early diagnosis of Alzheimer´s disease based on partial least squares, principal component analysis and support vector machine using segmented MRI images

**Article** *in* Neurocomputing · March 2015

DOI: 10.1016/j.neucom.2014.09.072

CITATIONS
70

READS
578

**5 authors**, including:

Laila Khedher
University of Granada
**12** PUBLICATIONS **120** CITATIONS
SEE PROFILE

Juan M Gorriz
University of Granada
**380** PUBLICATIONS **3,969** CITATIONS
SEE PROFILE

Abdelbasset Brahim
University of Granada
**14** PUBLICATIONS **126** CITATIONS
SEE PROFILE

# Early diagnosis of Alzheimer's disease based on Partial Least Squares, Principal Component Analysis and Support Vector Machine using segmented MRI images

L. Khedher[a], J. Ramírez[a], J.M. Górriz[a], A. Brahim[a], F. Segovia[a], and the Alzheimers Disease Neuroimaging Initiative[☆]

[a]*Dpt. Signal Theory, Networking and Communications. University of Granada, Spain.*

**Abstract**

Computer aided diagnosis (CAD) systems enable physicians to detect early stages of the Alzheimer's disease (AD), and structural magnetic resonance imaging (MRI) have been proved to be very useful in this task. This paper presents a new CAD system that improves the accuracy of the early AD diagnosis using tissue-segmented brain images. The proposed methodology to discriminate between AD, mild cognitive impairment (MCI) and elderly normal control (NC) subjects is based on multivariate approaches including partial least squares (PLS) and principal component analysis (PCA). In this study, 188 AD patients, 401 MCI patients and 229 control subjects from the Alzheimer's Disease Neuroimaging Initiative (ADNI) database were studied. Automated brain tissue segmentation was performed for each image obtaining gray matter (GM) and white matter (WM) tissue distributions. The validity of the analyzed methods was tested on the ADNI database by implementing support vector machine classifiers with linear or radial basis function (RBF) kernels to distinguish between the brain images of normal subjects and AD patients. Performance of our methodology is calculated using *k*-fold cross validation technique. Our system achieved good classification results using PLS feature extraction and linear SVM compared to PCA. In addition, PLS feature extraction is found to be more effective for extracting discriminative information from the data than PCA. The developed CAD system using PLS yielded maximum sensitivity, specificity and accuracy values of 85.11%, 91.27% and 88.49%, respectively.

*Keywords:* Computer Aided Diagnosis system, Alzheimer Disease, PLS, PCA, Support Vector Machine, ADNI database.

## 1. Introduction

Alzheimer's Disease (AD) is one of the most common forms of neurodegenerative brain disorders. This form of dementia is characterized by neurofibrillary tangles, amyloid plaques and histopathologic changes that are usually associated with neuronal loss and brain volume reductions [1]. This disease begins slowly, starting with memory loss and other cognitive functions getting worse until patients lose their ability to recognize very familiar things or persons. Furthermore, the occurrence and dominance of this disease will increase, in the coming years [2], due to the growth of the older population in developed nations. In addition, it is considered to be one of the major causes of death around the globe. Deaths from heart disease have decreased by 16%, breast cancer by 2%, prostate cancer by 8% and stroke by 23% whereas deaths by AD increased by 68% since year 2000 [3]. Up to now, the pathogenesis and pathologies of AD is unknown. In addition, there is still no special treatment for AD, hence early diagnosis becomes an important way to improve AD survival rate. To clinically diagnose AD at an early stage [4, 5], many biomedical imaging techniques have been used, such as Magnetic Resonance Imaging (MRI) [6, 7]. The MRI [6, 7] scan is a type of test that has been widely used for early detection and diagnosis of AD [4, 5, 8, 9, 10, 11]. This imaging

[☆]Data used in the preparation of this article were obtained from Alzheimers Disease Neuroimaging Initiative (ADNI)database (`www.loni.ucla.edu/ADNI`).As such, the investigators within the ADNI contributed to the design and implementation of ADNI and/or provided data but did not participate in analysis or writing of this report. ADNI investigators include (complete listing available at `www.loni.ucla.edu/ADNI/Collaboration/DNI_Manuscript_Citations.pdf`).

technique produces high quality images of the anatomical structures for the human body, specifically in the brain, and provides rich information for clinical diagnosis and biomedical research [12, 13]. The early changes are reliable with the underlying pathology of AD. However, it is unclear which structures are most useful for early diagnosis because the pattern of AD pathology is complex and evolves as the disease progresses [4]. Many studies have used manual delineation (segmentation) of the hippocampus in MR images [14, 15, 16, 17, 18, 19]. These studies have demonstrated a high accuracy in distinguishing between AD patients and normal controls. Automatic methods of measuring hippocampal volumes have also been applied with similar results [20, 21]. Entorhinal cortex measures have additionally been used to discriminate between subjects with AD and normal controls[15, 16]. Hippocampal volumes and entorhinal cortex measures have been found to be equally accurate in distinguishing between AD and normal cognitive elderly subjects [22]. It is probable that a single structure such as the hippocampus is not sufficient for accurate diagnosis of the disease and the combination of different structures has proven to be more useful when distinguishing AD patients from cognitively normal elderly subject [23]. Therefore, multivariate approaches give the opportunity to analyze many variables at the same time and observe the intrinsic patterns of the complex data from different regions of the brain. Previous studies have utilized different techniques of multivariate approaches such a Principal Component Analysis (PCA), Partial Least Square (PLS) and support vector machine (SVM) to analyze MRI data. In this work, we have used the PLS and PCA methods for analyzing our database. The aim of our study was to compare different feature extraction methods for classification of patients with AD, MCI and NC based on MRI segmented data (GM, WM and (GM+WM)).

This paper is organized as follows. In section 2 the database used to test the system, preprocessing technique, voxel selection, feature extraction methods, description of proposed methodology and classification methods used in this paper are presented. In section 3 we propose some experiments, and different results obtained with each combination are detailed. Discussion is given in section 4 in order to analyze the experimental results obtained in this work, and the conclusions are presented in the last section.

## 2. Materials and Methods

### *2.1. ADNI database*

The images used in this paper were obtained from the Alzheimer's Disease Neuroimaging Initiative(ADNI) (www.loni.ucla.edu/ADNI). ADNI was launched in 2003 by the National Institute on Aging (NIA), the National Institute of Biomedical Imaging and Bioengineering (NIBIB), the Food and Drug Administration (FDA), private pharmaceutical companies and non-profit organizations. The primary goal of ADNI has been to test whether serial magnetic resonance imaging (MRI), positron emission tomography (PET), other biological markers, and clinical and neuropsychological assessment can be combined to measure the progression of mild cognitive impairment (MCI) and early Alzheimer's disease (AD). Determination of sensitive and specific markers of very early AD progression is intended to aid researchers and clinicians to develop new treatments and monitor their effectiveness, as well as lessen the time and cost of clinical trials. The Principal Investigator of this initiative is Michael W. Weiner, MD, VA Medical Center and University of California  San Francisco. ADNI is the result of efforts of many co-investigators from a broad range of academic institutions and private corporations, and subjects have been recruited from over 50 sites across the U.S. and Canada. The initial goal of ADNI was to recruit 800 adults, ages 55–90, to participate in the research; approximately 200 cognitively normal older individuals to be followed for 3 years, 400 people with MCI to be followed for 3 years and 200 people with early AD to be followed for 2 years. For up-to-date information, see http://www.adni-info.org.

The ADNI database contains 1.5T and 3.0T t1w MRI scans for AD, MCI, and cognitively normal controls (NC) at several time points. In addition, all structural MR scans used in this paper were acquired at 1.5T MRI scanner and this database provides data for three groups of patients: healthy patients (Normal Controls, NC), Alzheimer disease patients (AD) and patients with mild cognitive symptoms (MCI). The database used in this work contains 1075 T1-weighted MRI images, comprising 229 NC, 401 MCI (312 stable MCI and 86 progressive MCI) and 188 AD. As only the first exam for each patient has been used in this work, 818 images were used for assessing the proposed approach. Demographic data of patients in the database is summarized in Table 1.

All subjects must be willing and able to undergo all test procedures including neuroimaging and agree to longitudinal follow-up. Specific psychoactive medications were excluded. General inclusion/exclusion criteria are as follows:

Table 1: Demographic data of patients in the database (ADNI 1075-T1)

| Diagnosis | Number | Age | Gender (M/F) | MMSE |
|---|---|---|---|---|
| NC | 229 | 75.97±5.0 | 119/110 | 29.00±1.0 |
| MCI | 401 | 74.85±7.4 | 258/143 | 27.01±1.8 |
| AD | 188 | 75.36±7.5 | 99/89 | 23.28±2.0 |

1. Normal control subjects: Mini-Mental State Examination (MMSE) (Folstein) scores between 24 and 30 (inclusive), a Clinical Dementia Rating (CDR) of 0, non depressed, non MCI, and non demented. The age range of normal subjects was roughly matched to that of MCI and AD subjects. Therefore, there should be minimal enrollment of normals under the age of 70.

2. MCI subjects: MMSE scores between 24 and 30 (inclusive), a memory complaint, objective memory loss measured by education adjusted scores on Wechsler Memory Scale Logical Memory II, a CDR of 0.5, absence of significant levels of impairment in other cognitive domains, essentially preserved activities of daily living, and an absence of dementia.

3. Mild AD subjects: MMSE scores between 20 and 26 (inclusive), CDR of 0.5 or 1.0, and meeting NINCDS/ADRDA [24] criteria for probable AD.

### *2.2. Image preprocessing*

MRI images from the ADNI database were preprocessed and segmented using the Statistical Parametric Mapping (SPM) software [25]. SPM was initially designed for functional images, but it also provides routines for realignment, smoothing and spatial normalization into a standard space of T1-weighted images. Moreover, the template from the VBF package [26] was used for this purpose. It is worth mentioning that normalization routines preserve the amount of tissues and not the intensities [25]. Thus, images from ADNI database were resized to 121×145×121 voxels with voxel sizes of 1.5 mm (sagital) x 1.5 mm (coronal) x 1.5 mm (axial). The segmentation performed by SPM provides probability maps for GM and WM, considering in values in the range (0,1) for each voxel, related to its membership probability.

### *2.3. Feature extraction methods*

Some dimension reduction techniques were applied to reduce the information contained in the brain images. In this sence, this section describes the methods for feature extraction used in this paper.

#### *2.3.1. Feature extraction based on Principal Component Analysis*

Principal component analysis (PCA) [27, 28] has been called one of the most important and valuable results from applied linear algebra (linear transformation). PCA is used frequently in all forms of analysis because it is an efficient tool for extracting the most significant features from a dataset. It is often used in neuroimaging in order to reduce the original high dimensional space of the brain images to a lower dimensional subspace [29, 30]. Furthermore, it has been successfully applied in neuroimage classification problems [31, 32].

Mathematically, PCA generates an orthonormal basis vector that maximizes the scatter of all the projected samples. After the preprocessing steps, the $n$ remaining voxels for each subject are rearranged into a vector form. Let $\mathbf{X} = [\mathbf{x_1}, \mathbf{x_2}..., \mathbf{x_N}]$ be the sample set of these vectors, where $N$ is the number of patients. After normalizing the vectors to unity norm and subtracting the large average, a new vector set $\mathbf{Y} = [\mathbf{y_1}, \mathbf{y_2}..., \mathbf{y_N}]$ is obtained, where each $\mathbf{y_i}$ represents an $n$-dimensional normalized vector, $\mathbf{y_i} = (y_{i1}, y_{i2}..., y_{in})^t$, $i = 1, 2, .., N$. The covariance matrix of the normalized vectors set is defined as:

$$\mathbf{\Sigma}_Y = \frac{1}{N}\sum_{n=1}^{N} \mathbf{y_i}\mathbf{y_i}^t = \frac{1}{N}\mathbf{Y}\mathbf{Y}^t \tag{1}$$

and the eigenvector and eigenvalue matrices $\mathbf{\Phi}$, $\mathbf{\Lambda}$ are computed as:

$$\mathbf{\Sigma}_Y \mathbf{\Phi} = \mathbf{\Phi}\mathbf{\Lambda} \tag{2}$$

Note that $\mathbf{Y}\mathbf{Y}^t$ is an $n \times n$ matrix while $\mathbf{Y}^t\mathbf{Y}$ is an $N \times N$ matrix. If the sample size $N$ is much smaller than the dimensionality $n$, then diagonalizing $\mathbf{Y}^t\mathbf{Y}$ instead of $\mathbf{Y}\mathbf{Y}^t$ reduces the computational complexity [15].

$$(\mathbf{Y}^t\mathbf{Y})\mathbf{\Psi} = \mathbf{\Psi}\mathbf{\Lambda_1} \tag{3}$$

$$\mathbf{T} = \mathbf{Y}\mathbf{\Psi} \tag{4}$$

where $\mathbf{\Lambda}_1$= diag$\{\lambda_1,\lambda_2,...,\lambda_N\}$ and $\mathbf{T}$=$[\mathbf{\Phi}_1,\mathbf{\Phi}_2,...,\mathbf{\Phi}_N]$. Derived from the eigenface concept[33], and due to its still brain-like appearance, the eigenvectors or principal components (PCs) $\mathbf{\Phi}_i$, $i = 1, 2, .., N$ of the covariance matrix are called eigenbrains [34]. Figure 1 shows the first four eigenbrains obtained from the ADNI database by the PCA algorithm.

(a) First eigenbrain (b) Second eigenbrain

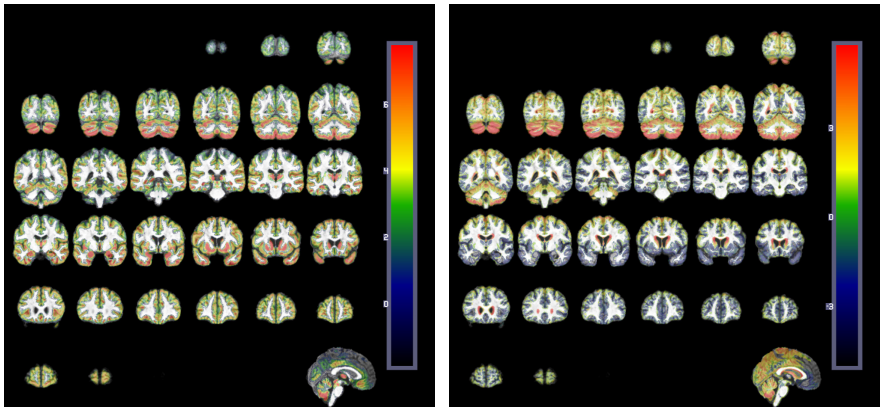

(c) Third eigenbrain (d) Fourth eigenbrain

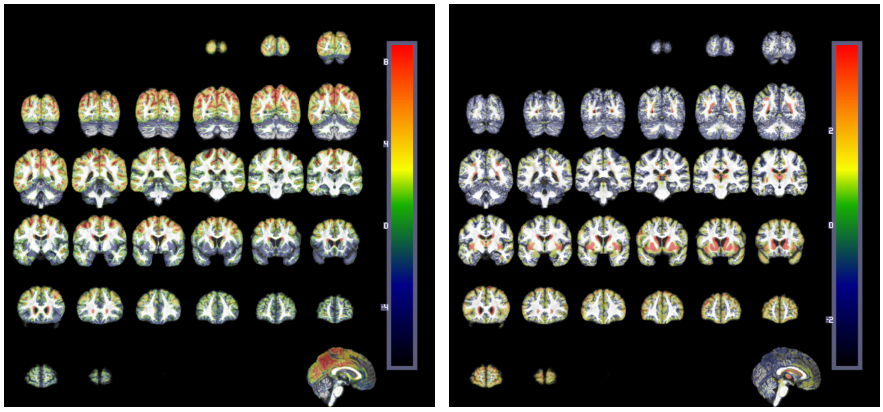

Figure 1: The first four Eigenbrains extracted from the ADNI database. They represent the principal components where original images will be projected onto to obtain a dimension reduction.

### *2.3.2. Feature extraction based on Partial Least Squares*

PLS [35, 36] is a statistical method that models sets of observed variables by means of latent variables. This method comprises regression and classification tasks as well as dimension reduction techniques and modeling tools.

The objective general of PLS is to maximize the covariance between different sets of variables. Both the predictor (the observed variables) and predicted (response) variables are considered as a block of variables. It finds a linear regression model by projecting the predicted variables and the observable variables to a new space. PLS can be used as a regression tool or as a dimension reduction technique similar to PCA [37, 38]. Mathematically, PLS is a linear algorithm that models the relation between two data sets: the observed variables $X \subset \mathbb{R}^{\mathbb{N}}$ (representing the feature space of input) and $Y \subset \mathbb{R}^{\mathbb{M}}$ (representing the labels). After observing $n$ data samples from each block of variables, PLS decomposes the $n \times N$ matrix of zero mean variables $\mathbf{X}$ and the $n \times M$ matrix of zero mean variables $\mathbf{Y}$ into the regression models form [39, 40]:

$$\mathbf{X} = \mathbf{T}\mathbf{P}^T + \mathbf{E} \tag{5}$$

$$\mathbf{Y} = \mathbf{U}\mathbf{Q}^T + \mathbf{F} \tag{6}$$

where $\mathbf{T}$ and $\mathbf{U}$ are $n \times p$ matrices of the $p$ extracted score vectors (components, latent vectors), the $N \times p$ matrix $\mathbf{P}$ and the $M \times p$ matrix $\mathbf{Q}$ represent matrices of loadings with number of columns being the number of PLS components and $n \times N$ matrix $\mathbf{E}$ and $n \times M$ matrix $\mathbf{F}$ are the matrices of residuals (or error matrices). The x-score in $\mathbf{T}$ are linear combinations of the x-variables, similarly, the y-score in $\mathbf{U}$ are linear combinations of the y-variables. The model

(a) First PLSbrain (b) Second PLSbrain

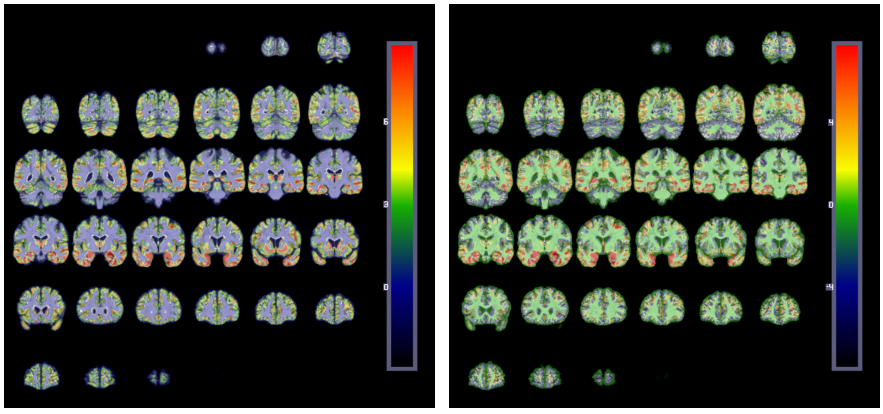

(c) Third PLSbrain (d) Fourth PLSbrain

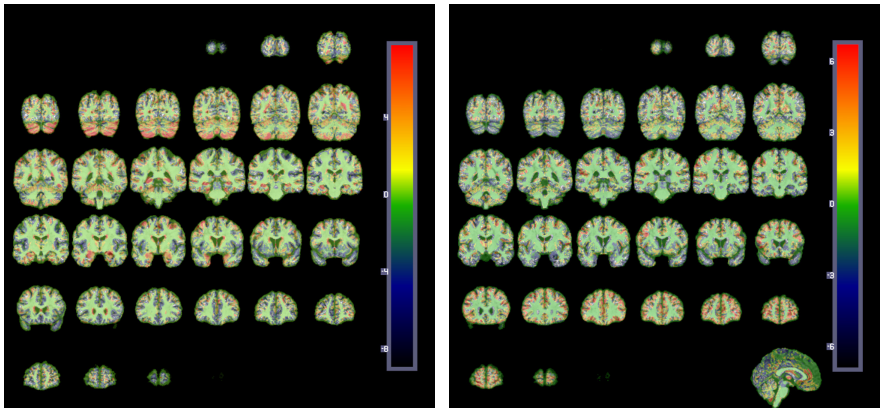

Figure 2: Representation of the four PLS-brain obtained by the PLS algorithm.

structure of PLS and PCA are the same in the sense that the data are first transformed into a set of a few intermediate linear latent variables (components) and these new variables are taken into account. The main difference between PLS

and PCA is that the former creates orthogonal weight vectors by maximizing the covariance between the variables **X** and **Y**. Thus, PLS not only considers the variance of the samples but also considers the class labels [35].

Both, PCA and PLS decompose the data into two sets of variables named scores and loadings. Thus, we can perform an interesting analysis based on the concept of eigenbrains (similar to the concept of eigenfaces [41] used in face recognition systems). That way, loadings would be viewed as elementary brain images and scores would represent the quantity of loadings used for building a specific image. The PLS-based methodology maximizes the covariance taking into account the labels information, thus the PLS-brains contain the differences between the two classes. In addition, most of the variance is gathered by the first components and therefore, most of the differences are also gathered by the first components. Figure 2 shows the representation of the first four PLS-brain obtained by the PLS algorithm.

### *2.4. Support vector machines classifier*

The support vector machine (SVM) is one of the more popular supervised learning algorithms that been applied to neuroimaging data in recent years [42, 43, 44, 45]. SVM demonstrates good classification performance, and is computationally efficient for training with high dimensional data. Besides, SVM represents a set of related supervised learning methods widely used in pattern recognition, voice activity detection, classification and regression analysis [46, 47, 48, 49]. It is introduced in order to separate a set of binary labeled training data with a hyperplane that is maximally distant from the two classes (called maximal margin hyperplane). The objective is to build a function $f$: $\mathbb{R}^N \rightarrow \pm 1$ using training data, that is, $n$-dimensional patterns $\mathbf{x_i}$ and class labels $y_i$, so that $f$ will correctly classify new examples $(\mathbf{x}, y)$:

$$(\mathbf{x_1}, y_1), (\mathbf{x_2}, y_2), ....., (\mathbf{x_N}, y_N) \in \mathbb{R}^N \times \pm 1 \tag{7}$$

Linear discriminant functions define decision hyperplanes in a multidimensional space, that is:

$$\mathbf{g(x)} = \mathbf{w}^{\mathrm{T}}\mathbf{x} + w_0 \tag{8}$$

where $\mathbf{w}$ is the weight vector that is orthogonal to the decision hyperplane and $w_0$ is the threshold. The optimization task consists of finding the unknown parameters $\mathbf{w_i}$, $i = 1, 2, .., N$ and $w_0$ that define the decision hyperplane. Let $\mathbf{x_i}$, $i = 1, 2, .., n$ be the feature vectors of the training set, $\mathbf{x}$. These belong to either of the two classes, $w_1$ or $w_2$. If the classes were linearly separable, the objective would be to design a hyperplane that classifies correctly all the training vectors. The hyperplane is not unique, and the selection process is focused on maximizing the generalization performance of the classifier, that is, the ability of the classifier, designed using the training set, to operate satisfactorily with new data. Among the different design criteria, the maximal margin hyperplane is usually selected since it leaves the maximum margin of separation between the two classes. Since the distance from a point $\mathbf{x}$ to the hyperplane is given by $z = |g(\mathbf{x})|/\|\mathbf{w}\|$, scaling w and $\mathbf{w_0}$ so that the value of $g(\mathbf{x})$ is +1 for the nearest point in $w_1$ and -1 for the nearest points in $w_2$, reduces the optimization problem to maximizing the margin: $2/\|\mathbf{w}\|$ with the constraints:

$$\mathbf{g(x)} = \mathbf{w^T x} + \mathbf{w_0} \geqslant 1, \forall \mathbf{x} \in w_1 \tag{9}$$

$$\mathbf{g(x)} = \mathbf{w^T x} + \mathbf{w_0} \leqslant 1, \forall \mathbf{x} \in w_2 \tag{10}$$

When no linear separation of the training data is possible, SVM can work effectively in combination with kernel techniques such as quadratic, polynomial or radial basis function (RBF), so that the hyperplane defining the SVM corresponds to a non-linear decision boundary in the input space [50]. A kernel function is defined as:

$$K(\mathbf{x_i}, \mathbf{x_j}) = \varphi(\mathbf{x_i})\varphi(\mathbf{x_j}) \tag{11}$$

The use of kernel functions avoids directly working in the high dimensional feature space, thus the training algorithm only depends on the data through dot products in Euclidean space, i.e., on terms of the form $\varphi(\mathbf{x_i})\varphi(\mathbf{x_j})$.

### 2.5. *Automated classification of AD based on PLS and PCA methods with SVM classifier*

A large number of CAD systems for AD are composed of three steps: (i) preprocessing procedure, (ii) feature extraction algorithm, and (iii) classification. The first step ensures that different images from different subjects, with brains of different size and shape, are comparable. The feature extraction algorithm transforms the input data into small vectors in order to avoid the small sample size problem [51]. These vectors must include all the relevant information contained in the input data. Once it has been trained, the classifier determines if they are more similar to healthy subject vectors , to MCI patient vectors or to AD patient vectors, thus performing the diagnosis.

In this work, we present a new classification approach for AD diagnosis which is based on segmented data (GM database and WM database) and a voxel selection process. This process reduces the input space dimensionality in order to address to the small sample size problem. Our developed CAD system consists as follows. Firstly, structural MRI images are normalized and segmented (preprocessing). Then, two binary masks are computed by averaging all the normal subjects for different segmented brain tissues datasets (WM and GM). Only the voxels that have an intensity above 10% of maximum intensity in the average image computed from control subjects in the GM database (the same for WM database), will be considered. This step reduces the number of voxels in the input space. For example, for data used in this work, the initial number of voxels per image (121×145×121=2122 945) is reduced to 382 325. Secondly, we apply a PLS or PCA algorithm to compute score vectors for selected voxels. These methods are efficient and robust, and have been successfully used to model complex data [52] and, even, to develop CAD system for AD. Finally, these vectors are used as input for a statistical classifier. In order to test this approach, we developed a CAD system for AD using a Support Vector Machine (SVM) classifier (Figure 3). It was used to estimate the underlying class (NC, MCI or AD) of each image. The performance of this system was estimated through a $k$-fold strategy.

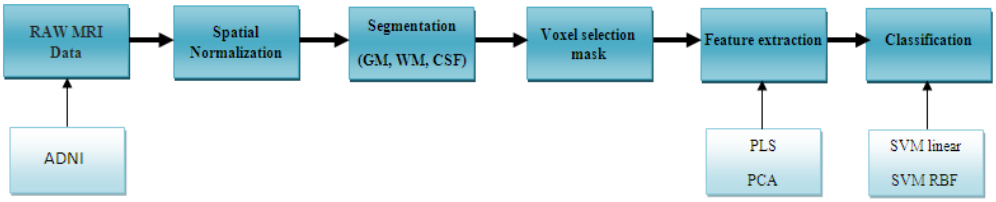


Figure 3: Detailed schema of the proposed CAD system.

## 3. Experiments and results

In this paper, a CAD system has been developed using two feature extraction methods and different SVM classifiers. Several performance metrics are estimated by using cross-validation. Apart from the well-known accuracy rate of a classification procedure, which computes the proportion between correctly classified samples and total samples, sensitivity and specificity are the most widely used parameters to describe a diagnosis test. The accuracy (Acc), sensitivity (Sens) and specificity (Spec) rates are defined as follows:

$$\text{Acc} = \frac{TP + TN}{TP + TN + TN + FP}, \qquad \text{Sens} = \frac{TP}{TP + FN}, \qquad \text{Spec} = \frac{TN}{TN + FP} \tag{12}$$

where $TP$ is the number of true positives: number of AD patients correctly classified; $TN$ is the number of true negatives: number of control subjects correctly classified; $FP$ is the number of false positives: number of control subjects classified as AD patients; $FN$ is the number of false negatives: number of AD patients classified as control subjects. Sensitivity and specificity are used to measure the proportion of actual positives or negatives which are identified correctly (e.g. the percentage of AD patients, or normal controls who are identified as such). These measures reveal the ability of a system to detect AD, MCI and NC patterns. Performance metrics are calculated using two cross-validation methods: $k$-fold cross validation and Leave-One-Out validation [53, 54]. $k$-fold has been used to assess the discriminative accuracy of different multivariate analysis methods applied to the discrimination of frontotemporal dementia from AD [25] and in classifying atrophy patterns based on MRI data [26]. It considers $k$ randomly selected

sets of AD patients, MCI and NC. It iteratively holds out a set for testing purposes, and train the classifier with the remaining sets, so that each set is left out once. This is repeated for all the $k$ sets, and an average value of the evaluation parameters is computed. Leave-One-Out is a particular case of $k$-fold, in which only one image is selected as test image.

In this work, two feature extraction methods (PCA and PLS) and two SVM classifiers (using linear or RBF kernel) were evaluated in order to develop more accurate CAD system for AD. Since our purpose is to distinguish between healthy subjects, MCI and AD patients, firstly, we trained the CAD system with only normal controls and AD images (group 1). Secondly, we have tested our system using MCI and AD images (group 2) and finally we have trained the CAD system with MCI and AD images (group 3). Tables 2, 3 and 4 show the statistical measures obtained using PLS and PCA methods. Also, performance of these feature extraction methods was calculated by means of $k$-fold cross validation with a number of folds equal to 10 ($k$=10).

### *3.1. Classification results for group 1 (NC vs. AD)*

In this section we present the classification results obtained in the first experiment, which consisted on distinguishing between NC and AD subjects. In this group, we test our method with all the database (229 NC, 401 MCI and 188 AD). Table 2 shows the values of the accuracy, sensitivity and specificity for the different brain tissues and compares different feature extraction methods and SVM classifiers. Linear SVM yielded higher accuracy rates for both PLS and PCA methods than RBF. Furthermore, when we compare the results obtained from PLS and PCA, we find that PLS feature extraction and linear kernel SVM yielded the best accuracy rates. Combining features extracted from GM and WM segmentation reported a classification accuracy of 88.49% for PLS and linear SVM (sensitivity=91.27% and specificity=85.11%) compared to 87.53% for GM only (sensitivity=88.65% and specificity=86.17%) and 85.61% for WM only (sensitivity=87.34% and specificity=83.51%). As a conclusion, combining features extracted from both GM and WM tissue distributions increases the classification and accuracy of the classifier.

Table 2: Statical measures of performances of the multivariate approach (PLS and PCA) for group 1 (NC vs AD), using 8 components for both features extraction techniques and two classifiers (SVM linear and RBF) with $k$=10.

| | PLS | | | PCA | | | |
|---|---|---|---|---|---|---|---|
| | Accuracy | Sensitivity | Specificity | Accuracy | Sensitivity | Specificity | |
| GM | 87.53% | 88.65 % | 86.17% | 85.61% | 89.08 % | 81.38% | SVM lin |
| WM | 85.61% | 87.34 % | 83.51% | 81.77% | 84.28 % | 78.72% | |
| (GM+WM) | 88.49% | 91.27 % | 85.11% | 87.77% | 89.96 % | 85.11% | |
| GM | 87.29% | 87.77 % | 86.70% | 83.93% | 86.26 % | 81.38% | SVM RBF |
| WM | 84.41% | 85.59 % | 82.98% | 81.29% | 83.41 % | 78.72% | |
| (GM+WM) | 88.49% | 90.39 % | 86.17% | 87.53% | 90.39 % | 84.04% | |

### *3.2. Classification results for group 2 (NC vs. MCI)*

The most difficult classification task concerning the ADNI database is to distinguish between NC and MCI patients, due to the wide range spanned by the features extracted from MCI patients. In this group, we have used only 370 MRI images (185 NC and 185 MCI subjects) from the ADNI database described in section 2.1. Using PLS and linear SVM, the combination of features extracted from GM and WM segmentation provided the highest accuracy, 81.89% (sensitivity=82.16% and specificity=81.62%), whereas the features extracted from GM or WM alone reported a classification accuracy of 77.57% and 80.54% respectively. Overall, we note that combining features extracted from both GM and WM tissue yielded the highest accuracy value. All results related to this classification model are reported in table 3.

Table 3: Statical measures of performances of the multivariate approach (PLS and PCA) for group 2 (NC vs MCI) using 8 components for both features extraction techniques and two classifiers (SVM linear and RBF) with k=10.

| | PLS | | | PCA | | | |
|---|---|---|---|---|---|---|---|
| | Accuracy | Sensitivity | Specificity | Accuracy | Sensitivity | Specificity | |
| GM | 77.57% | 76.76% | 71.90% | 75.41% | 78.38% | 72.43% | SVM lin |
| WM | 80.54% | 79.46% | 81.62% | 75.14% | 77.3% | 72.98% | |
| (GM+WM) | 81.89% | 82.16% | 81.62% | 78.92% | 80% | 77.84% | |
| GM | 76.22% | 81.62% | 70.81% | 72.97% | 75.68% | 70.27% | SVM RBF |
| WM | 81.35% | 76.22% | 80.54% | 72.70% | 64.86% | 80.54% | |
| (GM+WM) | 80.27% | 73.51% | 82.70% | 73.24% | 71.89% | 74.59% | |

### *3.3. Classification results for group 3 (MCI vs. AD)*

Table 4 shows the classification results obtained in the last experiment, which consisted on distinguishing between MCI and AD subjects using different SVM classifiers. Also, in this group we have used the same number of images as group 2. Combining features extracted from GM and WM segmentation reported a classification accuracy of 85.41% for PLS and linear SVM (sensitivity=87.03% and specificity=83.78%) compared to 77.03% for GM only (sensitivity=74.59% and specificity=79.46%)and 87.03% for WM only (sensitivity=88.65% and specificity=85.41%). These results showed that the most important change in the brain occurs more in the white matter than in the gray matter tissue brain[57].

Table 4: Statical measures of performances of the multivariate approach (PLS and PCA) for group 3 (MCI vs AD), using 8 components for both feature extraction techniques and two classifiers(SVM linear and RBF) with k=10.

| | PLS | | | PCA | | | |
|---|---|---|---|---|---|---|---|
| | Accuracy | Sensitivity | Specificity | Accuracy | Sensitivity | Specificity | |
| GM | 77.03% | 74.59% | 79.46% | 72.70% | 72.43% | 72.97% | SVM lin |
| WM | 87.03% | 88.65% | 85.41% | 79.19% | 82.16% | 76.22% | |
| (GM+WM) | 85.41% | 87.03% | 83.78% | 81.89% | 84.86% | 78.92% | |
| GM | 76.22% | 74.59% | 77.84% | 71.08% | 71.89% | 70.27% | SVM RBF |
| WM | 85.95% | 85.41% | 86.49% | 74.86% | 74.05% | 75.68% | |
| (GM+WM) | 85.41% | 85.95% | 84.86% | 76.77% | 74.59% | 78.92% | |

As shown in these tables, the both methods analyzed in this work highlight that the combination of features extracted from GM and WM tissue distributions give better accuracy, sensitivity and specificity than using different brain tissues separately. As a result, combining the different features extracted from both brain tissues (GM+WM) of patients with classification methods produces a valid approach to perform a CAD system for AD.

The accuracy of the different approaches depends on the size of the feature vector. For PLS and PCA based algorithm, the maximum size of the feature vectors is the number of images which are in database minus two. However, this number may be reduced by selecting only the most important components. Figure 4 shows the accuracy rates of the different groups achieved with both approaches in function of number of components selected (number of components=8).

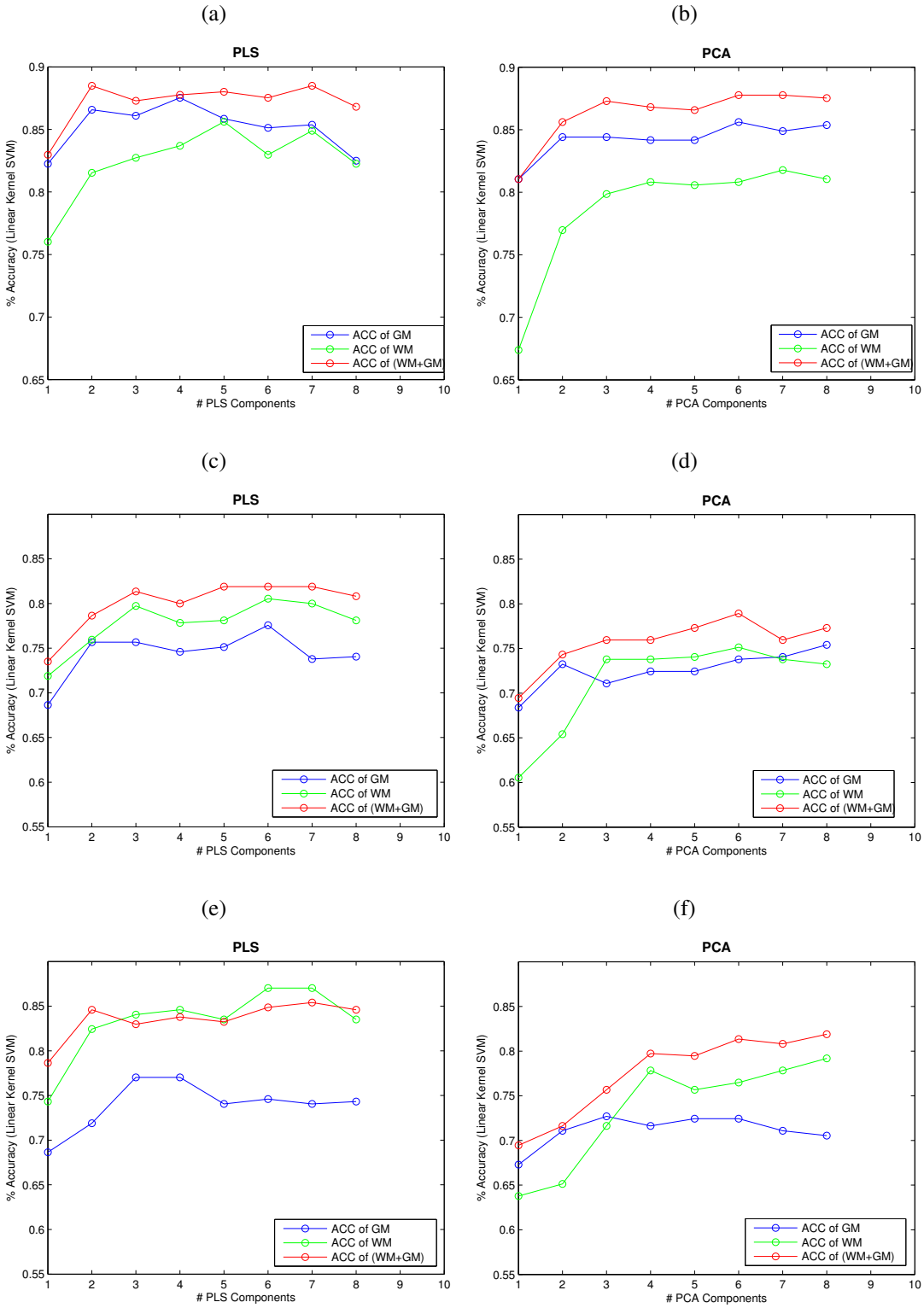


Figure 4: SVM classification: Values of Accuracy (%) computed for ADNI database in function of number of component for features extraction techniques PLS (left) and PCA (right):(a) and(b) are the results of group 1, (c) and (d) are the results of group 2, (e) and (f) are the results of group 3.

## 4. Discussion

As shown in section 3, the both methods analyzed in this paper are valid approaches to develop CAD system for AD. Besides, they achieve good values of accuracy, sensitivity and specificity. Figure 4 compares the classification performance of the PLS and PCA feature extraction methods with linear SVM classifier. Note that, the performance of the CAD system improves with the number of PCA or PLS components used as input features for classification which up to a maximum stable value. PLS outperforms PCA as a feature extraction technique yielding peak values of sensitivity = 91.27%, specificity = 85.11% and accuracy = 88.49% when compared to PCA that just yields sensitivity = 89.96%, specificity = 85.11% and accuracy = 87.77% (see figure 4 (a) and 4 (b)). The successful rate of PLS based method reached 88.49% for group 1. However, it is decreased for group 2 and 3 (78.92% ,85.4% respectively) when MCI images are included (see figure 4 (c) and 4 (d)). This is probably due to the high variability of the MCI pattern of each image. As a consequence, the classification task becomes more difficult (see Figure 5).

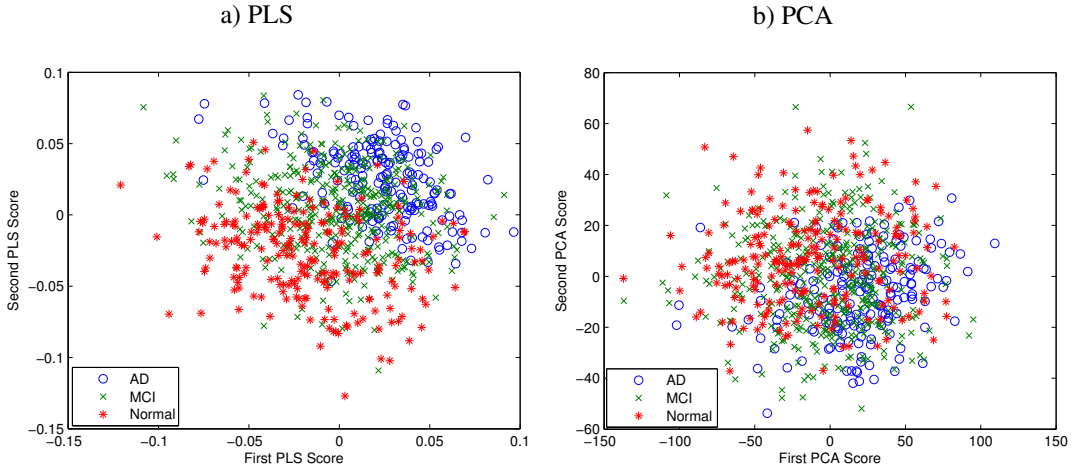


Figure 5: Representation of all images of the database using only the two first Scores of PLS and PCA.

As shown in figure 4 (c) and 4 (d), the classification result using only WM brain tissue is better than using only GM. This result confirms the previous study [55] in which the modification in the pattern of brain atrophy in early study (MCI) of disease occurs in the white matter tissue. Besides, elder subjects are likely to have WM structural abnormalities caused by leucoaraiosis or other diseases [56]. This abnormality in the WM brain tissue for patients with AD or MCI can make the structure very different from normal controls. Thus, the classification result in the WM can be better than in GM of brain images. Furthermore, the classification results for group 3 (see 4 (e) and 4 (f)) confirms that neurodegeneration starts in the WM and spreads to GM with the progression of the disorder.

It is worth noting that CAD systems are reproducing current medical knowledge since they have been trained with samples labeled by physicians. For this reason, statistical measures reported in this paper are an estimation about how a trained system is able to reproduce a medical diagnosis performed by experts [58]. Thus, some possible errors in the labeling process can modify the decision hyperplanes of the classifiers, specifically considering that the labels were assigned based on the scores obtained by patients in cognitive tests (as MMSE and CDR). In this work, we have previously shown that combining features extracted from GM and WM segmentation gives good classification accuracy using PLS and PCA methods. In addition, the PLS based method yields better classification results with smaller computational time than the PCA approach. The feature extraction approaches proposed in this paper achieve good classification performance when a linear SVM classifier is used. Furthermore, non linear classifiers like RBF require more samples or smaller feature vectors than linear classifier in order to give good classification results. A more interesting approach consists of selecting only some components of feature extraction methods, such as FDR as it is described in [32] and the Out-Of-Bag (OOB) error in [59].These previous methods achieve that using the first PCA/PLS components is optimal for classification purposes. In the development of our CAD system, we have selected only the 8 first PLS and PCA components. A higher number of components may worsen the classification results

since it increases the input space. In order to evaluate our CAD system, we use the receiver operating characteristic (ROC) curves. Figure 6 contains the sensitivity and 1-specificity values of the classification results in the ROC space considering the PLS and PCA techniques.

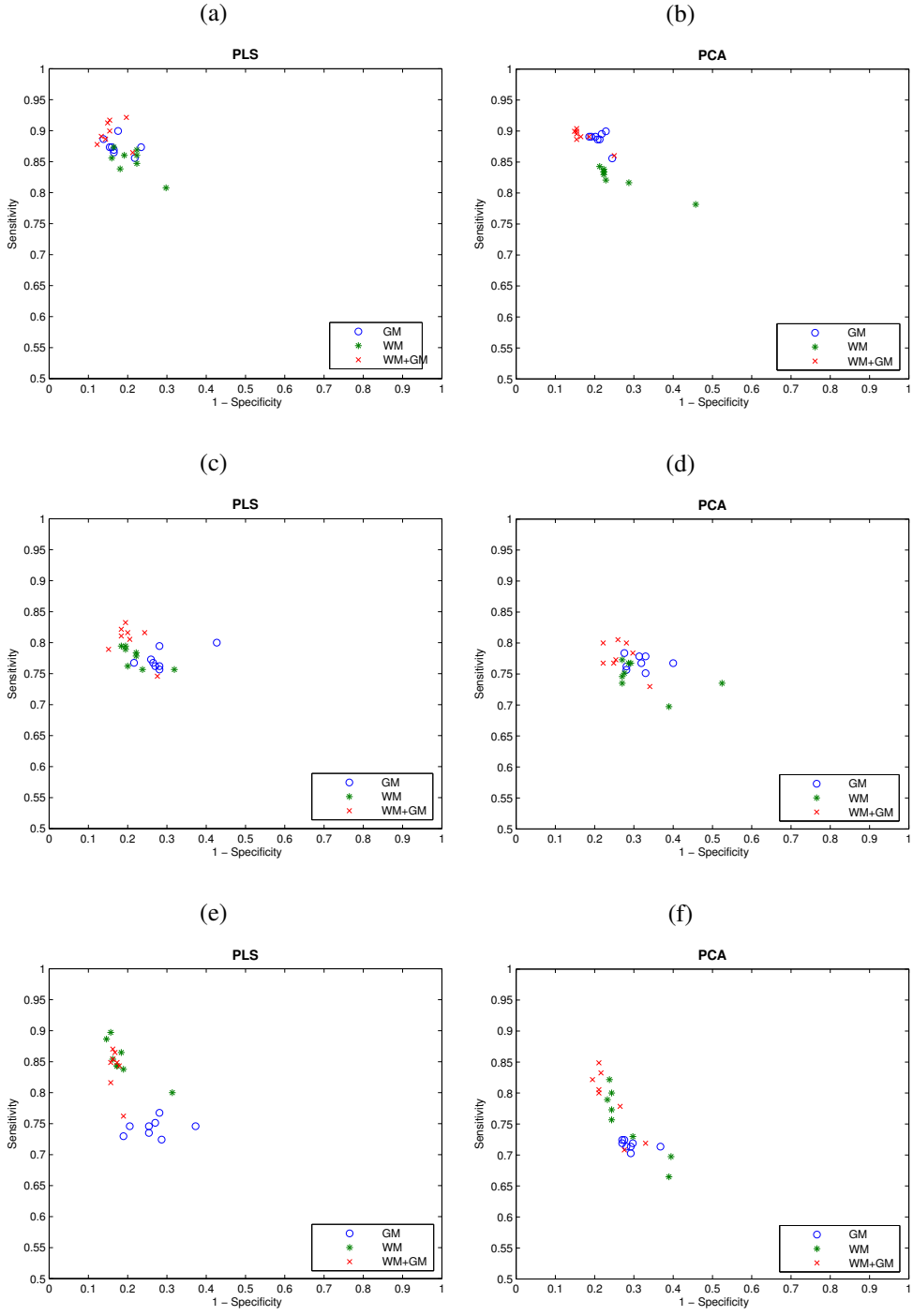


Figure 6: ROC curves for statistical measures obtained with different feature extraction methods using a linear classifier (SVM) for all ADNI images: Group 1((a) and (b)), group 2 ((c)and (d)) and group 3 ((e) and(f)).

These plots show a trade-off between the specificity and sensitivity of the CAD system when varying any of the input parameters. In addition, the closer to the left upper corner values are the better [60] (the combination of brain tissues, i.e. GM+WM).

## 5. Conclusion

A computer aided diagnosis system (CAD) for assisting the early detection of the Alzheimer's disease was shown in this paper. The system was developed by combining the different brain tissues and exploiting the two features extraction methods (PLS and PCA) in order to improve the classification of MRI images and to diagnose Alzheimer disease. The both multivariate approaches used in our proposed methodology allow the dimensionality reduction of the feature vector in order to surmount the small sample size problem. The difficulty arises in classification problems when the dimension of the feature vector is very high compared to the number of available samples. The PLS based method uses score vectors as features and performs with the PCA method an initial reduction of the input space by applying a binary mask according an intensity threshold that discard low intensity voxels. Both methods are tested with two classifiers (linear and RBF kernel) based on SVM. The resulting CAD system was based on segmented MRI images classification from the ADNI database. It was estimated using a $k$-fold cross validation methodology. The PLS method reached peak accuracy rate when we distinguish between controls and AD classes. In general, it outperforms several methods such as PCA approach.

## References


[1] Li. S, Shi. F, Pu. F, Li. X, Jiang. T, Xie. S and Wang. Y, Hippocampal Shape Analysis of Alzheimer Disease Based on Machine Learning Methods, AJNR Am J Neuroradiol 28 (7), 1339–1345, 2007.

[2] Brookmeyer. R, Johnson. E, Ziegler Graham. K, Arrighi. H, Forecasting the global burden of Alzheimers disease, Alzheimer's and Dementia 3 (3), 186–191, 2007.

[3] Alzheimer's Association, Alzheimer's disease facts and figures, Alzheimer's and Dementia 9 (2), 208–245, 2013.

[4] O'Brien. J.T, Role of imaging techniques in the diagnosis of dementia, Br. J. Radiol 80, 71–77, 2007.

[5] Ries. M.L, Carlsson. C.M, Rowley. H.A, Sager. M.A, Gleason. C.E, Asthana. S, Johnson. S.C, Magnetic resonance imaging characterization of brain structure and function in mild cognitive impairment, a review. J. Am. Geriatr. Soc 56, 920–934, 2008.

[6] Davatzikos. C, Fan. Y, Wu. X, Shen. D, Resnick. S.M, Detection of prodromal Alzheimer's disease via pattern classification of magnetic resonance imaging, Neurobiology of aging 29 (4), 514–523, 2008.

[7] Klppel. S, Stonnington. C.M, Chu. C, Draganski. B,Scahill. R.I, Rohrer. J.D, Fox. N.C, Jack. Jr C.R, Ashburner. J, Frackowiak. R.S.J, Automatic classification of MR scans in Alzheimer's disease, Brain 131 (3), 681–689, 2008.

[8] Fox. N.C, Cousens. S, Scahill. R, Harvey. R.J, Rossor. M.N, Using serial registered brain magnetic resonance imaging to measure disease progression in Alzheimer disease: Power calculations and estimates of sample size to detect treatment effects, Arch Neurol 57, 339–344, 2000.

[9] Jack. Jr C.R, Slomkowski. M, Gracon. S, Hoover. TM, Felmlee. JP, Stewart. K, Xu. Y, Shiung. M, O'Brien. P.C, Cha. R, Knopman. D, Petersen. R.C, MRI as a biomarker of disease progression in a therapeutic trial of milameline for AD. Neurology 60, 253–260, 2003.

[10] Scheltens. P, Fox. N, Barkhof. F, De Carli. C, Structural magnetic resonance imaging in the practical assessment of dementia: Beyond exclusion. Lancet Neurol 1, 13–21, 2002.

[11] Thompson. P.M, Hayashi. K.M, de Zubicaray. G, Janke. A.L, Rose. S.E, Semple. J, Herman. D, Hong. M.S, Dittmer. S.S, Doddrell. D.M, Toga. A.W, Dynamics of gray matter loss in Alzheimer's disease, J Neurosci 23, 994–1005, 2003.

[12] Zhang. Y, Wu. L, Wang. S, Magnetic resonance brain image classification by an improved artificial bee colony algorithm, Progress In Electromagnetics Research 116, 65–79, 2011.

[13] Oikonomou. A, Karanasiou. I.S, Uzunoglu. N.K, Phased-array near field radiometry for brain intracranial applications, Progress In Electromagnetics Research 109, 345–360, 2010.

[14] Fox. N.C, Warrington. E.K, Freeborough. P.A, Hartikainen. P, Kennedy. A.M, Stevens. J.M, Rossor. M.N, Presymptomatic hippocampal atrophy in Alzheimer's disease: A longitudinal MRI study. Brain 119, 2001–2007, 1996.

[15] Jack. Jr C.R, Petersen. R.C, Xu. Y.C, Waring. S.C, O'Brien. P.C, Tangalos. E.G, Smith. G.E, Ivnik. R.J, Kokmen. E, Medial temporal atrophy on MRI in normal aging and very mild Alzheimer's disease, Neurology 49, 786–794, 1997.

[16] Juottonen. K, Laakso. M.P, Partanen. K, Soininen. H, Comparative MR analysis of the entorhinal cortex and hippocampus in diagnosing Alzheimer disease, AJNR Am. J. Neuroradiol 20, 139–144, 1999.

[17] Killiany. R.J, Moss. M.B, Albert. M.S, Sandor. T, Tieman. J, Jolesz. F. Temporal lobe regions on magnetic resonance imaginimaging identify patients with early Alzheimer's disease, Arch. Neurol 50, 949–954, 1993.

[18] Laakso. M.P, Soininen. H, Partanen. K, Lehtovirta. M, Hallikainen. M, Hanninen. T, Helkala. E.L, Vainio. P, Riekkinen Sr. P.J, MRI of the hippocampus in Alzheimer's disease: sensitivity, specificity, and analysis of the incorrectly classified subjects, Neurobiol Aging 19 (1), 23–31, 1998.

[19] Lehericy. S, Baulac. M, Chiras. J, Pierot. L, Martin. N, Pillon. B, Deweer. B, Dubois. B,Marsault. C, Amygdalohippocampal MR volume measurements in the early stages of Alzheimer disease, AJNR Am. J. Neuroradiol 15, 929–937, 1994.

[20] Colliot. O, Chetelat. G, Chupin. M, Desgranges. B, Magnin. B, Benali. H, Dubois. B, Garnero. L, Eustache. F, Lehericy. S, Discrimination between Alzheimer disease, mild cognitive impairment, and normal aging by using automated segmentation of the hippocampus, Radiology 248 (1), 194–201, 2008.
[21] Morra. J.H, Tu. Z, Apostolova. L.G, Green. A.E, Avedissian. C, Madsen. S.K, Parikshak. N, Toga. A.W, Jack Jr. C.R, Schuff. N, Weiner. M.W, Thompson. P.M, Automated mapping of hippocampal atrophy in 1-year repeat MRI data from 490 subjects with Alzheimer's disease, mild cognitive impairment and elderly controls, Neuroimage, 2008.
[22] Kantarci. K, Magnetic resonance markers for early diagnosis and progression of Alzheimer's disease, Expert Review of Neurotherapeutics 5 (5), 663–670, 2005.
[23] Westman. E, Simmons. A, Zhang. Y, Muehlboeck. J.S, Tunnard. C, Liu. Y, Collins. L, Evans. A, Mecocci. P, Vellas. B, Tsolaki. M, Kloszewska. I, Soininen. H, Lovestone. S, Spenger. C, Wahlund. L.O, consortium. A, Multivariate analysis of MRI data for Alzheimer's disease, mild cognitive impairment and healthy controls, NeuroImage 54 (2), 1178–1187, 2011.
[24] McKhann. G, Drachman. D, Folstein. M, Katzman.R, Price. D, Stadlan. E.M, Clinical diagnosis of Alzheimer's disease: report of the NINCDS-ADRDA Work Groupa under the auspices of Department of Health and Human Services Task Force on Alzheimer's Disease, Neurology 34 (7), 939–944, 1984.
[25] Ashburner. J, Group T SPM8. Functional Imaging Laboratory, Institute of Neurology 12, Queen Square, Lonon WC1N 3BG, UK, 2011.
[26] Psychiatry SBMGD. Vbm toolboxes. University of Jena. URL http://dbm.neuro.uni-jena.de/vbm8/VBM8-Manual.pdf, 2013.
[27] Jolliffe. I, Principal Component Analysis, Springer Verlag, New York, 1986.
[28] . López. M, Ramírez. J, Górriz. J.M, Salas-Gonzalez. D, lvarez. I, Segovia. F, Automatic tool for the Alzheimers disease diagnosis using PCA and Bayesian classification rules, IET Electronics Letters 45 (8), 389–391, 2009.
[29] Andersen. A, Gash. D.M, Avison. M.J, Principal component analysis of the dynamic response measured by fMRI: a generalized linear systems framework, J.Magn.Reson.Imaging 17, 795–815, 1999.
[30] Yoon. U, Lee. J.M, Im. K, Shin. Y.W, Cho. B.H, Kim. I.Y, Kwon. J.S, Kim. S.I, Pattern classification using principal components of cortical thickness and its discriminative pattern in schizophrenia, NeuroImage 34, 1405–1415, 2007.
[31] López. M, Ramírez. J, Górriz. J.M, Salas-Gonzalez. D, Alvarez. I, Segovia. F, Puntonet. C.G, Automatic tool for the Alzheimers disease diagnosis using PCA and Bayesian classification rules, IET Electronics Letters 45 (8), 389–391, 2009.
[32] López. M, Ramírez. J, Górriz. J.M, Álvarez. I, Salas-Gonzalez. D, Segovia. F, Chaves. R, SVM-based cad system for early detection of the Alzheimers disease using kernel PCA and LDA, Neuroscience Letters 464 (4), 233–238, 2009.
[33] Turk. M, Pentland. A. Eigenfaces for recognition, Journal of Cognitive Neuroscience 3 (1), 71–86, 1991.
[34] Álvarez. I, Górriz. J.M, Ramírez. J, Salas-Gonzalez. D, López. M, Puntonet. C.G, Segovia. F, Alzheimer's diagnosis using eigenbrains and support vector machines, IET Electronics Letters 45 (7), 342–343, 2009.
[35] Wold. S, Ruhe. H, Wold. H, W.D. III, The collinearity problem in linear regression. The partial least squares (PLS) approach to generalized inverse, Journal of Scientific and Statistical Computations 5, 735–743, 1984.
[36] . Ramírez. J, Górriz. J.M, Segovia. F, Chaves. R, Salas-Gonzalez. D, López. M, Computer aided diagnosis system for the Alzheimers disease based on partial least squares and random forest SPECT image classification, Neuroscience Letters 472, 99–103, 2010.
[37] Nguyen. D.V, Rocke. D.M, Tumor classification by partial least squares using microarray gene expression data, Bioinformatics 18 (1), 39–50, 2002.
[38] Rosipal. R, Trejo. L.J, Kernel PLS-SVC for linear and nonlinear classification, in: Proceedings of the Twentieth International Conference on Machine Learning, 640–647, 2003.
[39] Ramírez. J, Górriz. J.M, Segovia. F, Chaves. R, Salas-Gonzalez. D, López. M, Illán. I, Padilla. P, Computer aided diagnosis system for the Alzheimer's disease based on partial least squares and random forest SPECT image classification, Neurosci Lett 472 (2), 99–103, 2010.
[40] Bastien. P, Vinzi. V.E, Tenenhaus. M, PLS generalised linear regression, Comput Stat Data Anal 48, 17–46, 2005.
[41] Turk. M, Pentland. A. Eigenfaces for recognition. Journal of Cognitive Neuroscience 3 (1), 71–86, 1991.
[42] Craddock. R.C, Holtzheimer III. P.E, Hu. X.P, Mayberg. H.S, Disease state prediction from resting state functional connectivity, Magn. Reson. Med 62, 1619–1628, 2009.
[43] Fan. Y, Resnick. S.M, Wu. X, Davatzikos. C, Structural and functional biomarkers of prodromal Alzheimer's disease: A high-dimensional pattern classification study, NeuroImage 41 (2), 277–285, 2008.
[44] Kloppel. S, Stonnington. C.M, Chu. C, Draganski. B, Scahill. R.I, Rohrer. J.D, Fox. N.C, Jack Jr. C.R, Ashburner. J, Frackowiak. R.S, Automatic classification of MR scans in Alzheimer's disease. Brain 131, 681–689, 2008.
[45] Mourao Miranda. J, Bokde. A.L, Born. C, Hampel. H, Stetter. M, Classifying brain states and determining the discriminating activation patterns: support vector machine on functional MRI data, NeuroImage 28, 980–995, 2005.
[46] Vapnik. V.N, Estimation of Dependences Based on Empirical Data, Springer Verlag, New York, 1982.
[47] Burges. C.J.C, A tutorial on support vector machines for pattern recognition, Data Mining and Knowledge Discovery 2 (2), 121–167, 1998 .
[48] Shawe-Taylor. J, Cristianini. N, Support Vector Machines and Other Kernel-Based, Learning Methods, Cambridge University Press, 2000.
[49] Scholkopf. B, Smola. A.J, Learning with Kernels. MIT Press, 2001.
[50] Chaves. R, Ramírez. J, Górriz. J.M, López. M, Salas Gonzalez. D, Alvarez. I, Segovia. F, SVM-based computer-aided diagnosis of the Alzheimer's disease using t-test NMSE feature selection with feature correlation weighting, Neurosci Lett 461, 293–297, 2009.
[51] Duin. R.P.W, Classifiers in almost empty spaces. Proceedings 15th international conference on pattern recognition, IEEE 2, 1–7, 2000.
[52] Wiklund. S, Johansson. E, Sjstrm. L, Mellerowicz. E.J, Edlund. U, Shockcor. J.P, Gottfries. J, Moritz. T , Trygg. J, Visualization of GC/TOF-MS-Based Metabolomics Data for Identification of Biochemically Interesting Compounds Using OPLS Class Models, Analytical Chemistry 80 (1), 115–122, 2008.
[53] Fan. Y, Shen. D, Davatzikos. C, Classification of structural images via highdimensional image warping, robust feature extraction, and SVM. Med ImagevComput Comput Assist Interv Int Conf Med Image Comput Comput Assist Interv 8, 1–8, 2005.
[54] Lao. Z, Shen. D, Xue. Z, Karacali. B, Resnick. S.M, Davatzikos. C, Morphological classification of brains via high-dimensional shape transformations and machine learning methods, NeuroImage 21 (1), 46–57, 2004.
[55] Gold. Brian T, Powell. David K, Andersen. Anders H, Smith. Charles D, Alterations in multiple measures of white matter integrity in normal

women at high risk for Alzheimer's disease, NeuroImage 52, 1487–1494, 2010.
[56] Cuingnet. Remi, Gerardin. Emilie, Tessieras. Jrme, Auzias. Guillaume, Lehricy. Stphane, Habert. Marie-Odile, Chupin. Marie, Benali. Habib, Colliot. Olivier and The Alzheimer's Disease Neuroimaging Initiative, Automatic classification of patients with Alzheimer's disease from structural MRI: A comparison of ten methods using the ADNI database, NeuroImage 56 (2), 766–81, 2011.
[57] Aikaterini. Xekardaki, Panteleimon. Giannakopoulos, Sven. Haller, White Matter Changes in Bipolar Disorder, Alzheimer Disease,and Mild Cognitive Impairment: New Insights from DTI, Journal of Aging Research 2011, 1–10, 2011.
[58] Segovia. F, Górriz. J.M, Ram´rez. J, Salas-Gonzalez. D, Álvarez. I, López. M, Chaves. R, The Alzheimers Disease Neuroimaging Initiative1, A comparative study of feature extraction methods for the diagnosis of Alzheimers disease using the ADNI database, Neurocomputing 75, 64–71, 2012.
[59] Segovia. F, Górriz. J.M, Ram´rez. J, Salas-Gonzalez. D, Álvarez. I, Early diagnosis of Alzheimers disease based on Partial Least Squares and Support Vector Machine, Expert Systems with Applications 40, 677–683, 2013.
[60] Metz. C, Basic Principles of ROC Analysis. Seminars Nucl Med 4 (8), 283–298, 1978.